MOLECULAR AND CELLULAR BIOLOGY, Dec. 1994, p. 7953–7966
0270-7306/94/$04.00+0

Vol. 14, No. 12

# $G_1$ Cyclin Degradation: the PEST Motif of Yeast Cln2 Is Necessary, but Not Sufficient, for Rapid Protein Turnover

SOFIE R. SALAMA, KRISTIN B. HENDRICKS, AND JEREMY THORNER*

*Department of Molecular and Cell Biology, Division of Biochemistry and Molecular Biology, University of California, Berkeley, California 94720-3202*

Received 27 May 1994/Returned for modification 28 June 1994/Accepted 31 August 1994

**The 545-residue Cln2 protein, like the other $G_1$ cyclins of *Saccharomyces cerevisiae*, is a very unstable protein. This instability is thought to play a critical role in regulating cell cycle progression. The carboxyl-terminal domains of Cln2 and the other $G_1$ cyclins contain sequences rich in Pro, Glu (and Asp), Ser, and Thr (so-called PEST motifs) that have been postulated to make up the signals that are responsible for the rapid degradation of these and other unstable proteins. To test this hypothesis, the carboxyl-terminal 178 residues of Cln2 were fused to the C terminus of a reporter enzyme, a truncated form of human thymidine kinase (hTKΔ40). The resulting chimeric protein (hTKΔ40-Cln2) retained thymidine kinase activity but was markedly less stable than hTK, hTKΔ40, or an hTK–β-galactosidase fusion protein, as judged by enzyme assay, immunoblotting with anti-hTK antibodies, pulse-chase analysis of the radiolabeled polypeptides, and ability to support the growth of a thymidylate auxotroph (*cdc21* mutant) on thymidine-containing medium. Thus, the presence of the Cln2 PEST domain was sufficient to destabilize a heterologous protein. Furthermore, the half-life of hTKΔ40-Cln2 was similar to that of authentic Cln2, and the rate of degradation of neither protein was detectably enhanced by treatments known to cause $G_1$ arrest, including exposure of *MAT*a haploids to α-factor mating pheromone and shifting *cdc28*$^{ts}$ and *cdc34*$^{ts}$ mutants to the restrictive temperature. These results suggest that the major signals responsible for Cln2 instability are confined to its C-terminal third. Because hTKΔ40-Cln2 and Cln2 were expressed from heterologous promoters yet their half-lives both in asynchronous cultures and when arrested at various cell cycle stages were always similar, the Cln2 PEST domain contains a signal for rapid protein turnover that is constitutively active and operative throughout the cell cycle. Removal of the 37 codons that encode the most prominent PEST-like segment from either hTKΔ40-Cln2 or Cln2 decreased the turnover rate of the resulting proteins, as expected; however, an hTKΔ40 chimera containing only this 37-residue segment was not detectably destabilized, suggesting that this PEST sequence, when removed from its normal context, is not a self-contained determinant of protein instability.**

In the budding yeast, *Saccharomyces cerevisiae*, commitment to a round of cell division occurs at a point late in the $G_1$ phase of the cell cycle (37). Progression through $G_1$ requires the action of a protein kinase, whose catalytic subunit is encoded by the *CDC28* gene (38, 59). Complexed to Cdc28 are proteins, termed $G_1$ cyclins, encoded by the *CLN1*, *CLN2*, and *CLN3* genes (8, 17, 31, 41). $G_1$ cyclin binding to p34$^{CDC28}$ is required for its activity both in vivo and in vitro (9, 56, 57, 60), and the requirement for a cyclin is a universal feature of the cell cycle-dependent protein kinases from a variety of other organisms (reviewed in references 36 and 52). p34$^{CDC28}$ is present at a relatively constant level throughout the cell cycle (30, 59); in contrast, the $G_1$ cyclins (especially Cln1 and Cln2) are present at high levels only in late $G_1$. This periodic expression of the $G_1$ cyclins is achieved, in part, by changes in the rate of synthesis of the corresponding mRNAs. This control is exerted via a potentiation mechanism involving phosphorylation (and activation) of the Swi4/Swi6 transcription factor responsible for stimulating *CLN1* and *CLN2* gene expression by p34$^{CDC28}$-$G_1$ cyclin complexes (reviewed in reference 32). However, for the level of a $G_1$ cyclin to be controlled primarily by its rate of synthesis, the protein must be turned over rapidly. Furthermore, after transit through $G_1$, the $G_1$ cyclins must be destroyed to permit association of p34$^{CDC28}$ with other cyclins that direct phosphorylation events required for the S and M phases of the cell cycle (32). As expected from these considerations, the $G_1$ cyclins are indeed very unstable proteins (41, 57, 60). Little is known, however, about the molecular determinants responsible for the instability of the $G_1$ cyclins.

Association of $G_1$ cyclins with p34$^{CDC28}$ appears to be rate limiting for transit through $G_1$ (reviewed in reference 39), just as the level of B-type cyclins is critical for passage through the M phase (reviewed in references 34 and 52). Mutations in *CLN2* (17) and *CLN3* (8, 31) that behave like dominant hyperactive alleles accelerate progression though $G_1$, resulting in a smaller than normal cell size and resistance to extracellular signals that normally impose $G_1$ arrest, including mating pheromone and nutrient limitation. Conversely, deletion of *CLN1* and *CLN2*, or *CLN3*, results in a larger than normal cell size because of delay in passage through $G_1$ (9, 17). Thus, proper modulation of $G_1$ cyclin levels is critical in *S. cerevisiae* for cell cycle progression, for the control of cell size, and for responsiveness to extracellular signals.

Degradation of mitotic (A- and B-type) cyclins is mediated via a conserved sequence motif that is found in their N-terminal domains and targets these proteins for polyubiquitination and subsequent proteolysis (13). However, the G1 cyclins lack this sequence element. The fact that the dominant hyperactive alleles (*CLN2-1*, *CLN3-1*, and *CLN3-2*) are all mutations which result in truncations that remove (or alter) the C-terminal third or so of these polypeptides suggested that this segment of each protein controls its stability. The C-

* Corresponding author. Mailing address: Department of Molecular and Cell Biology, Division of Biochemistry and Molecular Biology, University of California at Berkeley, Rm. 401, Barker Hall, Corner of Hearst & Oxford Sts., Berkeley, CA 94720-3202. Phone: (510) 642-2558. Fax: (510) 643-5035.

TABLE 1. *S. cerevisiae* strains used in this study

| Strain | Genotype | Source or reference |
|---|---|---|
| YPH499 | *MAT***a** *ade2-101*$^{oc}$ *his3-Δ200 leu2-Δ1 lys2-801*$^{am}$ *trp1-Δ1 ura3-52* | 51 |
| YPH500 | *MAT*α otherwise isogenic to YPH499 | 51 |
| DK499[a] | YPH499 *sst1-Δ5* | This laboratory |
| YSS4[b] | YPH499 *pho80::HIS3* | This work |
| 17026 | *MAT***a** *cdc21-1 ade1 ade2 gal1 his7 lys2 tyr1 ura1* [*rho*$^-$] | Yeast Genetic Stock Center[c] |
| YSS18[d] | *MAT*α *cdc21-1 ade his3-Δ200 LEU2 lys2 trp1-Δ63 ura3-52* | This work |
| YSS21[e] | *MAT***a** *cdc21-1 ade his3-Δ200 leu2-Δ1 lys2 pho80::HIS3 trp1-Δ63 ura3-52* | This work |
| YSS33[e] | *MAT***a** *cdc21-1 ade his3-Δ200 leu2-Δ1 lys2 trp1-Δ63 ura3-52* | This work |
| 4536-151 | *MAT*α *cdc15-1 ade3 can1 gal1 his7 leu2 sap3 ura1* | Doug Koshland[f] |
| YL10-1 | *MAT***a** *cdc34-2 GAL*$^+$ *his3-Δ200 leu2-Δ1 trp1-Δ63 ura3-52* | Mark Goebl[g] |

[a] The *sst1-Δ5::hisG/URA3/hisG* allele (40) was introduced into strain YPH499, and a Ura$^-$ derivative was selected on plates containing 5-fluoroorotic acid (5), as described by Reneke et al. (40) (23a).

[b] The *pho80::HIS3* allele (53) was introduced into strain YPH499 by DNA-mediated transformation, and genomic DNA from transformants with the appropriate phenotype (4) was examined by Southern blotting and hybridization analysis with an appropriate *PHO80* DNA probe to confirm integration of the disrupted allele at the *PHO80* locus.

[c] Yeast Genetic Stock Center, c/o R. K. Mortimer, Division of Genetics, Department of Molecular and Cell Biology, University of California, Donner Laboratory, Berkeley, Calif.

[d] Product of three successive backcrosses of strain 17026 against either YPH500 or YPH499, as appropriate.

[e] Product of a cross between YSS18 and YSS4.

[f] Doug Koshland, Department of Embryology, Carnegie Institution of Washington, Baltimore, Md.

[g] Mark Goebl, Department of Biochemistry and Molecular Biology, Indiana University-Purdue University School of Medicine, Indianapolis, Ind.

terminal domain of all three $G_1$ cyclins is rich in Pro, Glu (and Asp), Ser, and Thr—so-called PEST motifs—flanked by basic residues. Such PEST elements are found in many unstable proteins in eukaryotes, including the human C- and D-type cyclins (28), and have been postulated to be a signal that dictates rapid proteolysis (42). Consistent with this view, it has been reported that the truncated product of the *CLN3-1* allele is more stable than the normal Cln3 protein (57).

To examine whether major determinants for rapid protein turnover reside in the C-terminal domain of the $G_1$ cyclins, we investigated the ability of the C-terminal portion of Cln2 to confer instability on an otherwise very stable monomeric protein, specifically a truncated form (hTKΔ40) of human thymidine kinase (TK). We reasoned that hTK might be a useful reporter enzyme for this purpose for several reasons. First, hTK (27, 48) is an unstable protein in human cells and is degraded in a cell cycle-dependent manner (24, 49); however, like Cln2, the C-terminal portion of hTK is responsible for its instability because removal of just 40 residues from its C terminus, or attachment of heterologous sequences (for example, different parts of *Escherichia coli* LacZ), prevents the rapid degradation of hTK without detectably perturbing its enzymatic activity (24). Second, *S. cerevisiae* lacks any endogenous TK (2, 15), thereby permitting sensitive detection of a heterologously expressed TK. Finally, yeast strains which require TK activity for viability can be constructed (46, 47), thus providing a potential in vivo test of the stability of any hTK derivative.

Here we describe construction and expression in *S. cerevisiae* of an hTKΔ40-Cln2 chimera and various derivatives of this fusion. We used biochemical, immunological, and genetic methods to analyze the steady-state level and the rate of turnover of these proteins. In addition, as a means to demonstrate that degradation of the fusion protein accurately reflected the behavior of a bona fide $G_1$ cyclin, we analyzed the turnover of authentic Cln2 and examined the effect of various treatments and mutations that block cell cycle progression and that, hence, might operate by influencing the rate of degradation of the $G_1$ cyclins.

## MATERIALS AND METHODS

**Strains and culture conditions.** The yeast strains used in this work and their construction are described in Table 1. Strains were grown in a synthetic complete (SC) medium (50) containing 2% glucose as the carbon source but lacking either leucine or uracil for the maintenance of plasmids and enriched with (per liter) adenine sulfate (40 mg), L-His (60 mg), L-Lys (180 mg), L-Met (150 mg), L-Trp (80 mg), and either uracil (20 mg) (SCGlc-Leu medium) or L-Leu (225 mg) (SCGlc-Ura medium). In experiments requiring expression from the *GAL1* promoter, cells were pregrown in medium containing 2% raffinose as the carbon source and then galactose was added to a final concentration of 2%. To select for cells expressing TK, transformants of the *cdc21*$^{ts}$ strain were plated on SCGlc-Leu medium supplemented with 100 μg of thymidine per ml and incubated at the restrictive temperature (35°C). To radiolabel cells, cultures were pregrown in a synthetic minimal (SMM) medium (43) and [$^{35}$S]Cys and [$^{35}$S]Met were added. Cells were routinely grown at 30°C, except for strains carrying temperature-sensitive mutations, which were propagated at their permissive temperature (22 to 26°C).

**Recombinant DNA manipulations.** To generate multicopy (2μm DNA-based) plasmids that constitutively express hTK and its various derivatives in *S. cerevisiae*, the appropriate hTK constructs were inserted between the promoter and terminator of the *S. cerevisiae ADH1* gene in the vector pAD4M (29). A 932-bp *Sca*I-*Hin*dIII fragment containing the cDNA encoding the entire sequence of hTK plus 200 bp of its 3′-untranslated region was excised from pMGK24 (24) and inserted between the *Sma*I and *Sal*I sites of pAD4M to yield pSS3. An 813-bp *Sca*I-*Hin*dIII fragment containing a cDNA encoding hTKΔ40 plus 200 bp of its 3′-untranslated sequence was excised from pMGK606 (24) and inserted between the *Sma*I and *Sal*I sites of pAD4M to generate pSS4. The *Stu*I-*Sal*I segment of pSS3 was replaced with the *Stu*I-*Xba*I fragment from pMGK42, which contains the 3′ end of a cDNA encoding the hTK-LacZ60 fusion protein (24), to produce pSS10. Plasmid pSS9 was constructed in three steps. First, to position the *CLN2* coding sequence on the 3′ side of the hTK coding sequence, a 2.2-kb *Xho*I-*Xba*I fragment containing most of the *CLN2* gene

was inserted between the *Sac*I and *Sal*I sites in pSS3, yielding pSS8. Second, PCR was used to synthesize a 452-bp product that contained the precise in-frame junction between hTKΔ40 and the 178 C-terminal residues of Cln2 required to produce the *hTKΔ40-Cln2* chimeric gene. This product was generated by a three-primer method (61) with, as the templates, plasmids containing *hTK* (pSS3) and *CLN2* (pSS1). The latter plasmid is *CLN2* inserted into pRS313 (43b, 51). The 5′ primer (5′-ATC GACGAGGGGCAG-3′) corresponded to nucleotides 286 to 300 of *hTK*, the "joiner" oligonucleotide (5′-GTTCAAGTTG GATGCTGAGGCCTTCTTAAG-3′) corresponded to nucleotides 568 to 582 of *hTK* plus nucleotides 1447 to 1461 of *CLN2* (16), and the 3′ primer (5′-TTCCATATTCCGGCT-3′) corresponded to nucleotides 1603 to 1617 of *CLN2*. Finally, to generate *hTKΔ40-Cln2*, the 452-bp PCR product was digested with *Msc*I and *Sac*I and the resulting 375-bp fragment was substituted for the much larger *Msc*I-*Sac*I segment in pSS8, thereby producing pSS9. Construction of the correct fusion junction was confirmed by DNA sequence analysis by the dideoxynucleotide method (45).

PCR was also used to generate a construct (*hTKΔ40-Cln2ΔPEST*) containing a precise in-frame deletion of nucleotides 1462 to 1572 of *CLN2*, as follows. First, a 507-bp product was synthesized with pSS9 as the template, a 5′ primer (5′-GCACAGAGTTGATGA-3′) corresponding to nucleotides 98 to 112 of *hTK* (which is just upstream of a unique *Mlu*I restriction site), and a 3′ primer (5′-CGCGGAGCTCATGT TCAAGTTGGATGC-3′) corresponding to nucleotides 1447 to 1461 plus 1573 to 1580 of *CLN2* (which included a *Sac*I site from *Cln2* followed by four additional nucleotides). This product was cloned into the *Eco*RV site of pBluescriptKS$^+$ (Stratagene), and its sequence was confirmed. The *Mlu*I-*Sac*I fragment excised from the cloned PCR product was used to replace the larger *Mlu*I-*Sac*I segment in pSS9, thereby generating pSS13. PCR was also used to generate a construct (*hTKΔ40-Cln2PEST*) containing just the major PEST motif of Cln2 fused to the C terminus of hTKΔ40. A 624-bp product was synthesized with pSS9 as the template, the same 5′ primer used to construct pSS13 (see above), and a 3′ primer (5′-AGAGAGTGAGCTCATTTATCTCATTGGAGT-3′) corresponding to nucleotides 1558 to 1587 of *CLN2* but containing both a T-to-A substitution at position 1570 and a G-to-T substitution at position 1572 (which created a translational stop at codon 409 of *CLN2*). This product was cloned into the *Eco*RV site of pBluescriptKS$^+$, and its sequence was confirmed. The *Mlu*I-*Sac*I fragment excised from the cloned PCR product was used to replace the *Mlu*I-*Sac*I segment in pSS3, yielding pKBH2.

To permit high-level and regulated expression of Cln2, a 2.8-kb *Sph*I-*Xba*I fragment containing *CLN2* (excised from pSS1) was inserted into the *Sph*I and *Hin*dIII sites of the multicopy vector, YEp352GAL (1), to yield pSS25. To achieve galactose-dependent transcription of the *CLN2* coding sequence, the region between the *GAL1* promoter in YEp352 GAL and the initiator codon of *CLN2* was modified as follows. First, a 426-bp product containing a *Bam*HI site 30-bp upstream of the ATG of the *CLN2* open reading frame was synthesized by PCR with pSS1 as the template and a 5′ primer (5′-CTTACCGGATCCTAATTTGCATACAAAAG-3′) corresponding to nucleotides 270 to 298 of *CLN2* but with nucleotides 276 to 281 changed from 5′-ACATCA-3′ to 5′-GG ATCC-3′ and a 3′ primer (5′-TTTGGCTTGGTCCCG-3′) corresponding to nucleotides 682 to 696 of *CLN2*. This product was cloned into the *Eco*RV site of pBluescriptKS$^+$, and its sequence was confirmed. Finally, a 337-bp *Bam*HI-*Xho*I fragment excised from the cloned PCR product was substituted for the *Bam*HI-*Xho*I segment of pSS25, yielding pSS26. To generate a derivative of pSS26 containing a deletion of the major PEST motif (*CLN2ΔPEST*) identical to that removed in *hTKΔ40-Cln2ΔPEST*, PCR was performed with pSS26 as the template and a 5′ primer (5′-CCCAACCCAAGGGCACGT-3′) corresponding to nucleotides 798 to 816 of *CLN2* (which is just upstream of a unique *Spe*I site) and the same 3′ primer used in the construction of pSS13. The resulting 674-bp product was ligated into the *Eco*RV site of pBluescriptKS$^+$, and its sequence was confirmed. A 631-bp *Spe*I-*Sac*I fragment was excised from the cloned PCR product and used to replace the *Spe*I-*Sac*I segment of pSS26, producing pSS33. To express *CLN2ΔPEST* under control of the *CLN2* promoter on a low-copy-number (*CEN*) plasmid, the same 631-bp *Spe*I-*Sac*I fragment was used to replace the corresponding fragment in pSS1, producing pSS37. A truncation allele (*CLN2T*), which lacks the C-terminal 175 codons of *CLN2*, was constructed by using PCR to introduce two in-frame stop codons (-TAA TGA-) immediately following codon 370. For this purpose, a 672-bp product was generated with pSS1 as the template, the same 5′ primer as used in the construction of pSS33 (see above) and a 3′ primer (5′-CTCGAAATGTTCATTAGTTG GATGCA-3′), which corresponds to nucleotides 1446 to 1469 of *CLN2* but contains two extra T residues after position 1456 that result in the insertion of two extra A residues in the coding strand, thereby generating the first (TAA) of the two in-frame termination codons. This PCR product was ligated into the *Eco*RV site of pBluescriptKS$^+$, and its sequence was confirmed. Finally, the cloned PCR product was excised as a 646-bp *Spe*I-*Cla*I fragment and used to replace both the *Spe*I-*Cla*I fragment in pSS26, yielding pSS36, and the same segment in pSS1, generating pSS35.

All plasmids were introduced into *S. cerevisiae* by the lithium acetate method for DNA-mediated transformation (22). Standard methods and conventional *E. coli* strains were used for the propagation and isolation of plasmid DNAs (44).

**Antibodies.** Initially, the anti-hTK antibodies used in this study were a rabbit polyclonal antiserum (B3a) (48), generously provided by Thomas J. Kelly, Department of Molecular Biology and Genetics, Johns Hopkins University School of Medicine, Baltimore, Md. Subsequently, we raised other rabbit polyclonal anti-hTK sera as follows. A glutathione-*S*-transferase (GST)–hTK fusion was constructed by inserting a 900-bp *Sca*I-*Eco*RI fragment from pMGK28 (24) containing the entire hTK open reading frame into the *Sma*I and *Eco*RI sites of the vector, pGEX-3X (Pharmacia), creating pSS18. Cultures (50 ml) of *E. coli* DH5α harboring pSS18 were grown to stationary phase in Luria-Bertani broth supplemented with 100 μg of ampicillin per ml and used to inoculate larger cultures (1 liter) of the same medium. After growth for 1 h at 37°C, expression of GST-hTK was induced by addition of isopropyl-β-D-thiogalactopyranoside (IPTG) to a final concentration of 0.5 mM, and incubation at 37°C was continued for another 3 to 5 h. After being harvested by brief centrifugation, the cells were washed once with Tris-buffered saline (TBS; 150 mM NaCl, 50 mM Tris-HCl [pH 7.5]), resuspended in 20 ml of TBS, and lysed by sonication. The lysate was adjusted to a final concentration of 1% Triton X-100, agitated on a roller drum for 20 min at 4°C, and clarified by centrifugation at 27,000 × *g* for 20 min. The resulting supernatant solution was mixed with 1 ml of preswollen glutathione-agarose beads (Sigma) for 2 h at 4°C on a roller drum. The mixture was poured into a column (0.9 by 8 cm), washed with 50 volumes of TBS plus 0.2% Triton-X100, and eluted with TBS plus 0.2% Triton-X100 containing 5 mM glutathione. The peak fractions, as judged by $A_{280}$, were pooled, examined by sodium dodecyl sulfate-poly-

acrylamide gel electrophoresis (SDS-PAGE), and used for immunization of two adult female New Zealand White rabbits (initial injections were 1 mg of GST-hTK emulsified in complete Freund's adjuvant, and booster immunizations were 0.1 mg of GST-hTK emulsified in incomplete Freund's adjuvant, administered at 4- to 6-week intervals). Blood was drawn 10 to 14 days after each immunization and tested by immunoblotting (54) against yeast extracts expressing hTK and hTKΔ40. The anti-hTK antibodies in one antiserum (antiserum 693) were purified by immunoaffinity adsorption as follows. A sample (2 mg) of GST-hTK (prepared as described above) was coupled to 0.2 ml of activated agarose beads (Affi-Gel 10; Bio-Rad) as specified by the manufacturer. Crude antiserum was clarified by sedimentation for 2 min in a microcentrifuge, and the supernatant solution was diluted 1:10 in TBS. The diluted serum was passed successively three times over a column (0.9 by 8 cm) containing the GST-hTK-agarose beads. The bed was washed with 50 volumes of TBS and 20 volumes of 50 mM Tris-HCl (pH 7.5) containing 500 mM NaCl and then eluted with 0.2 M glycine (pH 2.0). Fractions (400 μl) were collected into tubes containing 100 μl of Tris-HCl (pH 9.1). Peak fractions (as measured by both $A_{280}$ and the ability to recognize hTK and hTKΔ40 on immunoblots) were pooled, adjusted to a final concentration of 1% bovine serum albumin, and stored in aliquots at −20°C.

To prepare rabbit polyclonal anti-Cln2 antibodies, a TrpE-Cln2 fusion was constructed by inserting a 700-bp *Xho*I-*Bam*HI fragment from pBKK1, which is a partial *CLN2* clone in pBluescript-KS and encodes residues 89 to 320 of Cln2 (provided by Karl Kuchler, this laboratory), into the vector, pATH21 (25). The fusion protein was expressed in *E. coli* DH5α, purified from inclusion bodies, and used for immunization of rabbits as described previously (26). The immunoglobulin G fraction was purified from one anti-Cln2 antiserum (antiserum 9010) by ammonium sulfate precipitation and batch treatment with DEAE-cellulose, as described in detail elsewhere (18).

**Preparation of cell extracts, TK assays, and immunoblotting.** Cultures of YPH499 harboring various hTK constructs or the parent vector (pAD4M) were grown to an $A_{600}$ of 1.0 in SCGlc-Leu at 30°C. Cells were harvested by brief centrifugation, and equal portions (equivalent to 500 $A_{600}$ units) of each culture were washed by resuspension and recentrifugation in ice-cold TK buffer (190 mM Tris-HCl [pH 7.5], 1.9 mM $MgCl_2$). The washed pellets were resuspended in 0.5 ml of TK buffer containing 1 mM dithiothreitol and 0.5 mM phenylmethylsulfonyl fluoride, lysed by seven 30-s pulses of vigorous vortex mixing in the presence of 0.5 g of acid-washed glass beads (diameter, 0.45 to 0.5 mm), and clarified by centrifugation at 7,000 × *g* for 6 min. The resulting cell-free homogenate was decanted and further clarified by centrifugation at 100,000 × *g* for 30 min. The final clarified supernatant fraction was divided into aliquots, which were immediately frozen in liquid $N_2$ and stored at −80°C until used. The protein concentration in each extract (which ranged from 10 to 20 mg/ml) was determined with a commercial protein assay kit (Bio-Rad) as specified by the manufacturer.

TK (ATP:thymidine 5′-phosphotransferase; EC 2.7.1.21) activity was measured by monitoring the ATP-dependent conversion of [*methyl*-$^3$H]thymidine to dTMP. The reaction mixture (27, 48) contained, in a final volume of 100 μl, TK assay buffer (190 mM Tris-HCl [pH 7.5], 1.9 mM $MgCl_2$, 0.1% bovine serum albumin, 2.5% glycerol, 10 mM dithiothreitol, 10 mM NaF), 22 μM [*methyl*-$^3$H]thymidine (910 mCi/mmol), and an ATP-regenerating system consisting of 1.9 mM ATP, 3 mM phosphocreatine, and 6.75 μg of creatine kinase per ml. Reactions were initiated by the addition of extract, incubated for 30 min at 37°C, and terminated by spotting a sample (50 μl) onto a filter disk (diameter, 2.3 cm) of DEAE-cellulose (Whatman DE81). The disks were placed in a suspended basket in a 500-ml beaker, washed (for 5 min each) with one change of $H_2O$ and three changes of 95% ethanol, air dried, placed in plastic vials containing 5 ml of a liquid scintillation fluid (Packard Scint-AXF), and counted in a liquid scintillation spectrometer (Beckman LS7500).

For immunodetection of hTK, samples (10 μg of total protein) of yeast extracts, prepared as described above, were diluted into gel sample buffer (67 mM Tris-HCl [pH 6.8], 0.67 mM EDTA, 2% SDS, 6.7% glycerol, 0.02% bromphenol blue), heated at 95°C for 5 min, and then subjected to SDS-PAGE (12.5% polyacrylamide) (10). The resolved proteins were transferred to a nitrocellulose filter (Schleicher & Schüll BA83; pore size, 0.2 μm) by standard procedures (54). The filters were incubated with a 1:2,000 dilution of a polyclonal rabbit anti-hTK serum (antiserum B3a) (49), and the immune complexes formed were detected with a horseradish peroxidase-conjugated goat anti-rabbit secondary antibody and a chemiluminescence detection system (ECL; Amersham) under the conditions recommended by the supplier.

**Radiolabeling and immunoprecipitation.** Yeast cells were radiolabeled essentially as described by Hosobuchi et al. (21). Cultures of YPH499 harboring various plasmids were grown overnight in SMM containing 100 μM $(NH_4)_2SO_4$ to an $A_{600}$ of 0.2 to 0.4. Cells were collected by centrifugation and resuspended in sulfate-free SMM at a concentration (per milliliter) equivalent to an $A_{600}$ of 5. After preincubation for 15 min at 30°C, a mixture of [$^{35}$S]Met and [$^{35}$S]Cys (Tran$^{35}$S-Label; ICN) (30 μCi/$A_{600}$ unit) was added, and incubation was continued for another 10 min. A chase was then initiated by addition of 1/100 volume of 0.3% L-Cys–0.4% L-Met–100 mM $(NH_4)_2SO_4$, and samples (equivalent to 2 $A_{600}$ units) were removed at various times and quenched by mixing with an equal volume of ice-cold 20 mM $NaN_3$. After being washed once with 10 mM $NaN_3$, the azide-killed cells were resuspended in 300 μl of lysis buffer (50 mM Tris-HCl [pH 7.5], 1% SDS, 1 mM EDTA, 1 mM phenylmethylsulfonyl fluoride), mixed with glass beads (~0.5 g), and lysed by vigorous vortex mixing for 90 s followed by heating at 95°C for 5 min. The lysate was transferred to a fresh tube via a 200-μl flat-ended white plastic Pipetman tip, mixed with 900 μl of phosphate-buffered saline containing 1% Triton X-100 and 50 μl of a slurry of fixed *Staphylococcus aureus* cells (IgGsorb; The Enzyme Center), and clarified by centrifugation for 10 min in a microcentrifuge. The supernatant fraction was typically stored at −20°C before use.

For immunoprecipitation of hTK-related antigens, samples ($10^7$ cpm total) of each extract were diluted to a final volume of 1 ml in IP buffer (150 mM NaCl, 1% Triton X-100, 0.1% SDS, 15 mM Tris-HCl [pH 7.5], 2 mM $NaN_3$) supplemented with additional SDS to a final concentration of 0.2%, and the hTK-related antigens were collected by incubation overnight at 4°C with a sample (5 μl) of either whole-rabbit polyclonal anti-hTK serum (antiserum B3a) (49) or a sample (10 μl) of a solution of the affinity-purified rabbit anti-hTK antibodies prepared in this laboratory (see above) plus 25 μl of a 20% suspension of protein A-Sepharose CL4B beads (Pharmacia). The protein A-containing beads were collected by brief sedimentation in a microcentrifuge and washed by successive resuspension and recentrifugation, as follows: twice in IP buffer, twice in 2 M urea–200 mM NaCl–2 mM $NaN_3$–1% Triton X-100–100 mM Tris-HCl (pH 7.5), twice in IP buffer containing 500 mM NaCl, and once in 50 mM NaCl–2 mM $NaN_3$–10 mM Tris-HCl (pH 7.5). The protein A-containing

beads were then resuspended in SDS-PAGE sample buffer (20 μl) and heated at 95°C for 5 min, and the resulting eluate was subjected to SDS-PAGE in a 12.5% polyacrylamide gel and visualized by autoradiography on Kodak X-Omat AR film. Strains expressing *CLN2* constructs were radiolabeled as above, with the following modifications. Cultures were pregrown with raffinose as the carbon source (instead of glucose), and, 2 h prior to initiation of radiolabeling, galactose (final concentration, 2%) was added to the cultures to induce synthesis of Cln2. For pulse-chase experiments in which the effect of addition of α-factor (final concentration, $6 \times 10^{-7}$ M) was examined, DK499 (*MAT***a** *sst1-Δ5*) was used to prevent extracellular degradation of the pheromone. The pheromone was added either 10 or 30 min before initiation of radiolabeling. For pulse-chase experiments in which the effect of temperature-sensitive mutations was examined YL10-1 (*cdc34-2$^{ts}$*), YSS33 (*cdc21-1$^{ts}$*), 453615-1 (*cdc15-1$^{ts}$*), and several strains carrying different *cdc28$^{ts}$* alleles were pregrown at 26°C. At 2 h prior to initiation of radiolabeling, the culture was split into two equal portions. One sample was shifted to 37°C for the remainder of the experiment, and the other sample was maintained at 26°C. For immunoprecipitation of Cln2-related antigens, samples of each extract ($10^6$ cpm total) were incubated in the presence of a sample (8 μl) of a solution of the immunoglobulin G fraction purified from a rabbit polyclonal anti-Cln2 antiserum (see above) and treated as described above for hTK-related antigens.

To calculate an approximate half-life for each hTK and Cln2 construct, the amount of radioactivity remaining at each time point after initiation of the chase was quantified with a PhosphorImager (Molecular Dynamics, Sunnyvale, Calif.) and the logarithm of the values so obtained were plotted versus time (see Fig. 7 and 8). Each datum point represents the average of at least three independent trials. Since the decay curves were monotonic but nonlinear, it was assumed that first-order kinetics were followed between the zero time point and the two earliest time points of the chase period (5 and 15 min), an approach used by others under similar circumstances (20). Lines were fitted by a least-squares program.

## RESULTS

**The hTKΔ40-Cln2 chimera is a functional enzyme.** PCR was used to fuse the 178 C-terminal codons of *CLN2* in frame to a hTK cDNA lacking its C-terminal 40 codons, creating the chimeric gene *hTKΔ40-CLN2*. The segment of Cln2 fused (residues 368 to 545) corresponds almost exactly to the sequence removed in the *CLN2-1* mutation (17) and includes the major putative PEST motif (Fig. 1A). For expression in *S. cerevisiae* the hTKΔ40-Cln2 fusion and control constructs encoding full-length hTK, hTKΔ40, or an hTK-LacZ chimera (24) were inserted between the promoter and terminator of the *S. cerevisiae ADH1* gene in a multicopy vector, thereby generating pSS9, pSS3, pSS4, and pSS10, respectively (Fig. 1B). These plasmids were introduced into the same recipient strain by DNA-mediated transformation, and the level of expression of each construct was measured in several ways.

To determine whether the transcript levels of the various hTK constructs were similar, total RNA was extracted from each transformant, resolved by agarose gel electrophoresis, transferred to a nitrocellulose filter, and hybridized to a hTK probe. Within the resolution of this method, the transcripts encoding hTK, hTKΔ40, and hTKΔ40-Cln2 (hTK-LacZ60 was not examined) were all expressed at equivalent levels (data not shown). To determine whether the corresponding proteins were functional enzymes, extracts of transformants expressing

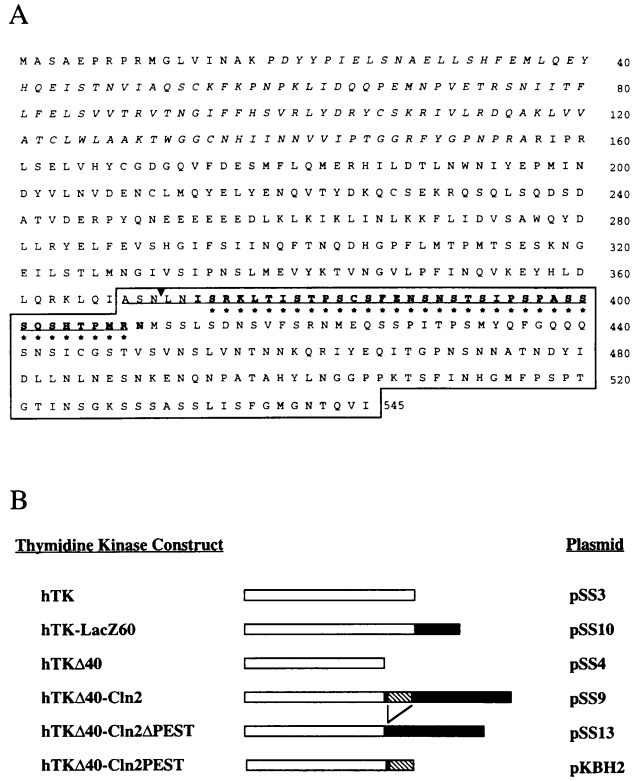


FIG. 1. Primary sequence of Cln2 and schematic representation of the hTK constructs. (A) Deduced amino acid sequence of the *CLN2* gene product in the one-letter code. Amino acids in italics (residues 18 to 156) indicate the cyclin box, a region of homology to other cyclins (16, 17). The boxed amino acids (residues 368 to 545) represent the portion of Cln2 that was fused to the C-terminal end of hTKΔ40 to generate hTKΔ40-Cln2. Residues within the box marked by an asterisk below represent the major PEST-like segment, according to the formula of Rogers et al. (42), and residues shown in bold type are those that were deleted to generate hTKΔ40-Cln2ΔPEST and Cln2ΔPEST. Residues underlined correspond to those present in hTKΔ40-Cln2PEST. Arrowhead indicates the position at which the coding sequence was truncated to generate Cln2T. (B) Plasmids expressing hTK and derivatives. Each construction (left), diagrammed schematically (middle), was inserted between the promoter and terminator of the constitutively expressed *S. cerevisiae ADH1* gene in the expression vector pAD4M (29), which also contains the *LEU2* gene for selection, thereby generating the set of plasmids (right) used in this study. pSS3 contains full-length hTK, and pSS4 contains a derivative of hTK that lacks its 40 C-terminal amino acids. pSS10 contains a chimeric gene in which the amino-terminal 60 amino acids of *E. coli* β-galactosidase (LacZ) have been fused in frame to the C terminus of full-length hTK. pSS9 contains a chimeric gene in which residues 368 to 545 of Cln2 have been fused in frame to the C terminus of hTKΔ40. pSS13 is identical to pSS9, except that the sequence corresponding to codons 373 to 409 of *CLN2* have been removed by a precise in-frame deletion. pKBH2 contains codons 368 to 408 of *CLN2* fused in frame to *hTKΔ40*. Open rectangles are hTK sequence, gray rectangle is LacZ sequence, solid rectangles are Cln2 sequence, and hatched rectangles are the major PEST segment.

each of the constructs were prepared and assayed for TK activity in vitro. Cells carrying vector alone had no detectable TK activity, as expected from previous findings (2, 15), whereas cells expressing hTK and hTKΔ40, or hTK-LacZ60 (data not shown) had readily detectable enzyme levels (Fig. 2). Furthermore, the specific activities of extracts expressing either hTK or hTKΔ40 were virtually identical, and that from cells express-

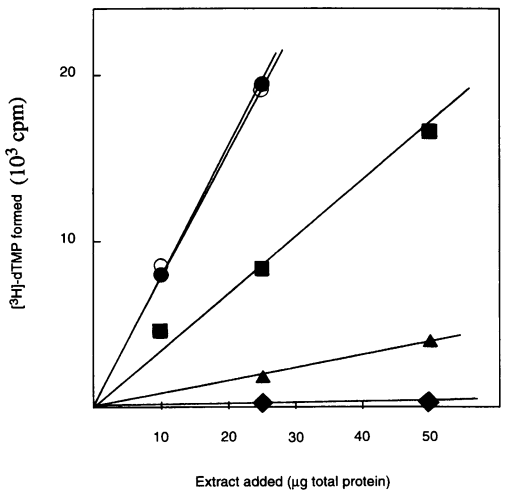


FIG. 2. TK activity of strains expressing hTK and hTK derivatives. Cytosolic extracts of a yeast strain (YPH499) containing a plasmid expressing either hTK (solid circles), hTKΔ40 (open circles), hTKΔ40-Cln2ΔPEST (squares), hTKΔ40-Cln2 (triangles), or vector alone (diamonds) were assayed for TK activity by measuring the ATP-dependent conversion of [*methyl*-$^3$H]TdR to dTMP, as described in Materials and Methods. Each datum point represents the average of reactions performed in duplicate.

ing hTK-LacZ60 was also essentially the same (data not shown). In contrast, extracts from cells expressing hTKΔ40-Cln2 had a markedly lower (as much as 10-fold), but still detectable, level of TK activity (Fig. 2).

Because extracts from cells expressing hTK-LacZ60 had a specific activity indistinguishable from that of extracts of cells expressing hTK or hTKΔ40, the lower specific activity found in extracts of cells expressing hTKΔ40-Cln2 was most probably due to a lower steady-state level of the chimeric protein (rather than due to inhibition of the catalytic activity of the enzyme resulting from the presence of additional C-terminal sequences per se). To address this issue directly, equal amounts of protein from the same extracts were resolved by PAGE, transferred to a nitrocellulose filter, incubated with rabbit polyclonal anti-hTK antibodies, and visualized with a chemiluminescence detection system. In agreement with the enzyme assays, this immunological analysis (Fig. 3) showed that the amount of the hTKΔ40-Cln2 polypeptide present (lane 5) was much smaller (at least fivefold) than the amount of the hTK (lanes 1 and 4) and hTKΔ40 (lane 2) proteins or hTK-LacZ60 (data not shown), as estimated from a comparison of the exposure times required to generate bands of equivalent intensity. These results indicated that hTKΔ40-Cln2 is an active enzyme but that the presence of the Cln2 sequence caused the chimeric protein to be degraded more rapidly, resulting in its low steady-state level compared with hTK, hTKΔ40, and hTK-LacZ60.

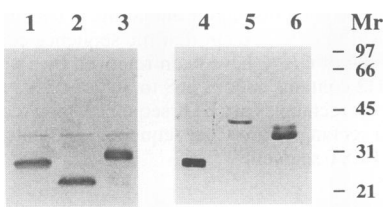


FIG. 3. Steady-state levels of hTK and hTK derivatives. Cytosolic extracts of a yeast strain (YPH499) containing a plasmid expressing either hTK (lanes 1 and 4), hTKΔ40 (lane 2), hTKΔ40-Cln2PEST (lane 3), hTKΔ40-Cln2 (lane 5), or hTKΔ40-Cln2ΔPEST (lane 6) were prepared. An equivalent amount (10 μg) of each extract was loaded in each lane, subjected to SDS-PAGE, and transferred electrophoretically to a nitrocellulose filter, and the filter replica was probed with anti-hTK antibodies, as described in Materials and Methods.

**The hTKΔ40-Cln2 chimera has a very short half-life.** To directly monitor the rate of degradation of these proteins in vivo, pulse-chase experiments were performed. Cells expressing hTK or hTKΔ40-Cln2 were radiolabeled with [$^{35}$S]Met and [$^{35}$S]Cys briefly and then shifted to medium containing excess nonradioactive Met and Cys. At various times thereafter, cell samples were withdrawn, lysed, subjected to immunoprecipitation with anti-hTK antiserum, and analyzed by PAGE and autoradiography. When analyzed in this way, hTK was completely stable for at least 2 h after initiation of the chase (Fig. 4A). In agreement with the results of enzyme assays (Fig. 2) and immunoblot analysis (Fig. 3), pulse-chase experiments also showed that both hTKΔ40 and hTK-LacZ60 were just as stable as hTK itself over the 2-h time course (data not shown). In dramatic contrast, hTKΔ40-Cln2 was very rapidly degraded (Fig. 4B). As estimated from its initial rate of decay (see Materials and Methods), the approximate half-life of hTKΔ40-Cln2 was 12 min (see Fig. 6A). This result confirmed that the presence of the Cln2 sequence resulted in a chimeric protein with a very high rate of turnover. Thus, the nature of the Cln2 sequence, and not the mere presence of additional C-terminal residues, was responsible for the instability of the hTKΔ40-Cln2 chimera.

**The half-life of the hTKΔ40-Cln2 chimera is similar to that of authentic Cln2.** The steady-state level of Cln2 corresponds very closely to the level of transcription of its cognate gene, suggesting that Cln2 is a very unstable protein (60). Indeed, the endogenous level of Cln2 is just at the limit of detection when rabbit polyclonal anti-Cln2 antibodies are used (60) and is difficult to detect even when tagged with epitopes from the c-Myc oncoprotein (43a) or the influenza virus hemagglutinin (56). Hence, to examine the rate of turnover of Cln2 by pulse-chase analysis to compare its stability with that of hTKΔ40-Cln2, the *CLN2* gene was overexpressed. For this purpose, a plasmid (p*GAL1-CLN2*) expressing *CLN2* under control of the inducible *GAL1* promoter was constructed. Transformants carrying this plasmid were shifted to galactose medium 2 h prior to initiation of the pulse-chase regimen to induce Cln2 expression, and Cln2-related antigens were immunoprecipitated from extracts prepared from samples withdrawn at various times during the chase by using the immunoglobulin G fraction purified from a rabbit polyclonal antiserum raised against a TrpE-Cln2 fusion protein (see Materials and Methods). As expected, Cln2 was degraded very rapidly (Fig. 5A), with an approximate half-life of 8 min (Fig. 6B). Thus, within the resolution of these methods, the half-life of hTKΔ40-Cln2 was very similar to that of authentic Cln2, suggesting that the primary determinants of the instability of Cln2 reside within its C-terminal domain.

**Role of PEST sequences in Cln2 instability.** To specifically investigate the contribution of the PEST sequences in the 178-residue carboxyl-terminal region of Cln2 to the instability displayed by hTKΔ40-Cln2, the most PEST-like 37 codons (Fig. 1A) were deleted from the *hTKΔ40-CLN2* coding sequence to generate *hTKΔ40-Cln2ΔPEST*. This construction was inserted into the same expression vector as the other hTK derivatives, yielding plasmid pSS13 (Fig. 1B). As judged both by the specific activity of TK in extracts of cells producing hTKΔ40-Cln2ΔPEST (Fig. 2) and by the amount of the

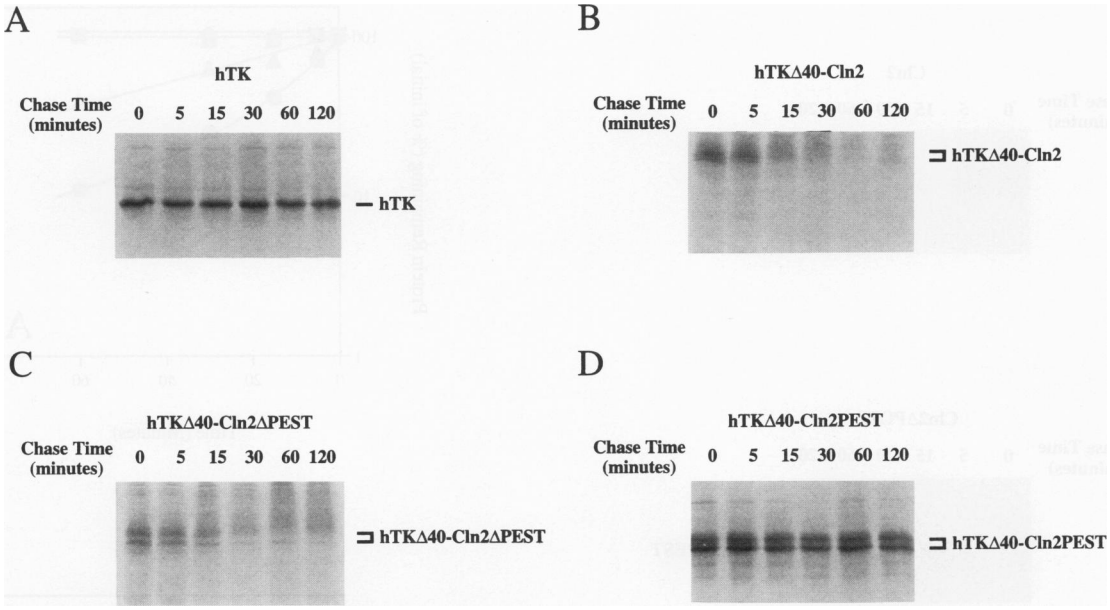


FIG. 4. Pulse-chase analysis of the turnover of hTK and hTK derivatives. A yeast strain (YPH499) expressing either hTK (A), hTKΔ40-Cln2 (B), hTKΔ40-Cln2ΔPEST (C), or hTKΔ40-Cln2PEST (D) was radiolabeled with [$^{35}$S]Cys and [$^{35}$S]Met for 10 min. After addition of excess unlabeled Cys, Met, and free $SO_4^{2-}$, cell samples were withdrawn at the indicated times and extracts were prepared. hTK-related antigens were immunoprecipitated from these extracts with anti-hTK antibodies and analyzed by SDS-PAGE and autoradiography, as described in Materials and Methods.

hTKΔ40-Cln2ΔPEST polypeptide detected by immunoblotting (Fig. 3), the removal of this 37-residue segment significantly increased the steady-state level of the chimeric protein.

To look directly at the effect of removing the major PEST segment on the degradation rate of hTKΔ40-Cln2ΔPEST, pulse-chase analysis was performed on cells expressing this construct (Fig. 4C). In agreement with the increase in the steady-state level of hTKΔ40-Cln2ΔPEST observed by biochemical and immunological tests, removal of the PEST segment significantly enhanced the stability of the protein, increasing its half-life nearly threefold (Fig. 6A). Although removal of the major PEST element significantly extended the half-life of the chimeric protein, its stability was still substantially lower than that of hTK, suggesting that additional, perhaps redundant, signals for rapid degradation reside within the portion of the Cln2 tail that remains in hTKΔ40-Cln2ΔPEST.

To examine the contribution of this PEST element to the instability of authentic Cln2, the identical 37-codon deletion that was made in *hTKΔ40-CLN2ΔPEST* was also introduced into the *CLN2* coding sequence in the p*GAL1-CLN2* expression plasmid. The turnover of the protein produced from p*GAL1-CLN2ΔPEST* was then examined by pulse-chase analysis in transformants expressing this construction. Consistent with the effect of removal of this PEST segment from hTKΔ40-Cln2, Cln2ΔPEST was significantly more stable than Cln2 (Fig. 5B). However, this stabilization was more pronounced at later time points (Fig. 6B), since the absence of this PEST element reduced the initial rate of turnover of Cln2 only modestly (about twofold). This result again suggests that within the 141 residues of the C-terminal tail remaining in Cln2ΔPEST there are likely to be additional determinants which contribute to the instability of the protein.

These considerations prompted us to examine the stability of a complete truncation of Cln2 that lacks its 175 C-terminal residues, which we designated Cln2T. To try to create such a mutation, Hadwiger et al. (17) subcloned a *Sal*I-*Hin*dIII fragment from their original isolate and inserted it into another vector. While this manuever cleaved the *CLN2* coding sequence at an internal *Hin*dIII site that resides immediately after codon 375, it inadvertently resulted in the joining of the *CLN2* sequence in frame to vector sequences, thereby creating an allele (*CLN2-1*) that specifies a readthrough protein, rather than a precise truncation (58a). To avoid this problem, we used PCR to create two in-frame stop codons immediately following codon 370 (Fig. 1A), as described in Materials and Methods. As determined by pulse-chase analysis (Fig. 5C), the Cln2T protein was only slightly more stable then Cln2ΔPEST with regard to its initial rate of decay (Fig. 6B); however, at later times (60 to 120 min after the chase), the Cln2T protein persisted detectably (Fig. 5C) whereas the Cln2ΔPEST disappeared (Fig. 5B). The fact that Cln2T is indeed a more stable protein than Cln2ΔPEST was confirmed by an independent in vivo assay. To minimize any effects of long-term overproduction of these proteins, constructs expressing Cln2, Cln2ΔPEST, and Cln2T were introduced into *MAT***a** cells on low-copy-number (*CEN*) plasmids under control of the normal *CLN2* promoter. The transformants were then challenged with α-factor mating pheromone by the standard halo bioassay (40). Cells carrying the vector alone gave the expected clear haloes as a result of their growth arrest in $G_1$ (Fig. 7A). Cells expressing normal Cln2 produced only slightly smaller haloes than the control, and these were also essentially clear (Fig. 7B). In contrast, cells expressing Cln2ΔPEST displayed distinctly smaller haloes than the control, and these haloes were uniformly turbid, because of the rapid resumption of cell cycling after the initial arrest in response to pheromone (Fig. 7C). Most strikingly, the cells expressing Cln2T gave barely adumbrated haloes, indicating that they were almost completely resistant to the growth-arresting effect of the pheromone (Fig.

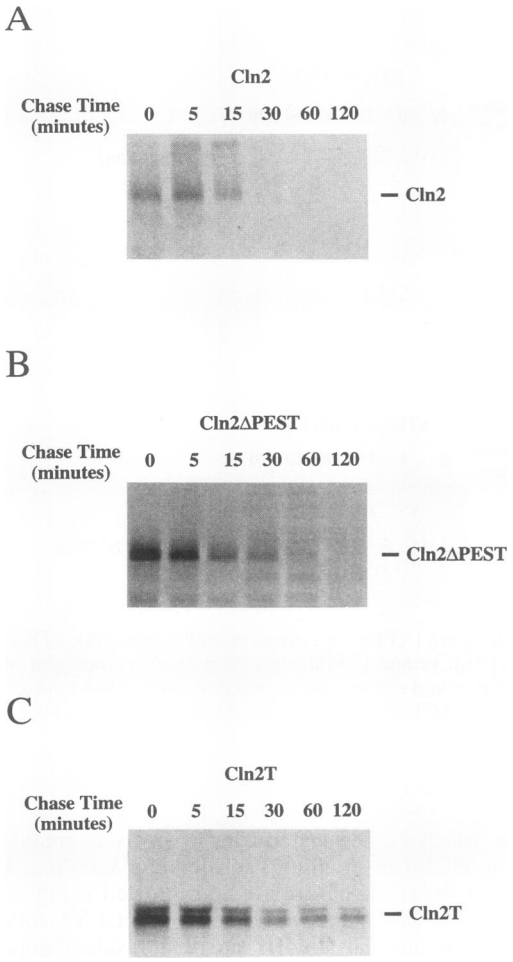


FIG. 5. Pulse-chase analysis of the turnover of Cln2 and Cln2 derivatives. A yeast strain (YPH499) expressing either Cln2 (A), Cln2ΔPEST (B), or Cln2T (C) was radiolabeled with [$^{35}$S]Cys and [$^{35}$S]Met for 10 min. After addition of excess unlabeled Cys, Met, and free $SO_4^{2-}$, cell samples were withdrawn at the indicated times and extracts were prepared. Cln2-related antigens were immunoprecipitated from these extracts with anti-Cln2 antibodies and analyzed by SDS-PAGE and autoradiography, as described in Materials and Methods.

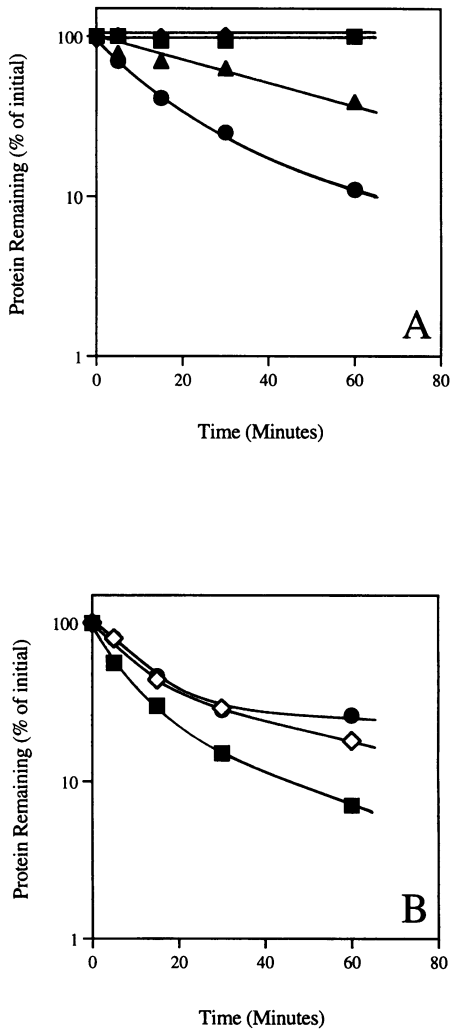


FIG. 6. Half-lives of hTK, Cln2, and derivatives. (A) Comparison of the degradation rate of hTK and hTK derivatives. Symbols: squares, hTK; diamonds, hTK-Cln2PEST; triangles, hTKΔ40-Cln2ΔPEST; circles, hTKΔ40-Cln2. (B) Comparison of the degradation rate of Cln2 and Cln2 derivatives. Symbols: squares, Cln2; diamonds, Cln2ΔPEST; circles, Cln2T. Approximate half-lives based on these plots were calculated as described in Materials and Methods.

7D), as had been reported previously for the *CLN2-1* allele (17). Thus, the response to α factor was graded in inverse relationship to the stability of the Cln2 derivative examined. These results suggest that the C-terminal third of Cln2 contains determinants of instability in addition to the major PEST element removed in Cln2ΔPEST.

Nonetheless, because removal of the major putative PEST motif was able to enhance significantly the stability of both Cln2 and the hTKΔ40-Cln2 chimera, this segment is clearly necessary for the maximum rate of turnover of both proteins. To determine if this PEST sequence could act as an isolated element to confer instability independently from its context within the Cln2 tail, we introduced a translational termination signal into *hTKΔ40-CLN2* at codon 409 of the Cln2 coding sequence, which is immediately downstream of the major PEST motif (Fig. 1A), thereby generating *hTKΔ40-Cln2PEST* (Fig. 1B). Somewhat unexpectedly, immunoblot analysis indicated that the steady-state level of the product of this construction, hTKΔ40-Cln2PEST, was as high as that of hTK and hTKΔ40 (Fig. 3), and pulse-chase analysis confirmed that the stability of hTKΔ40-Cln2PEST was indistinguishable from that of hTK (Fig. 4D and 6A). This result indicates that, while the major PEST sequence is necessary for the characteristic instability of Cln2, it is not sufficient to target a protein for rapid destruction.

**Degradation of hTKΔ40-Cln2 and Cln2 is a constitutive process.** The rate of turnover of both Cln2 and hTKΔ40-Cln2 was determined by pulse-chase analysis with plasmid constructs that placed the expression of each of these proteins under the control of a heterologous promoter (*GAL1* and *ADH1*, respectively), thereby uncoupling their expression from cell cycle events. Hence, a corollary of the fact that both polypeptides were degraded rapidly in asynchronous cultures is that the machinery responsible for their recognition and destruction must be present constitutively and operative throughout the cell cycle. On the other hand, another group who expressed *CLN2* from a constitutive promoter reported

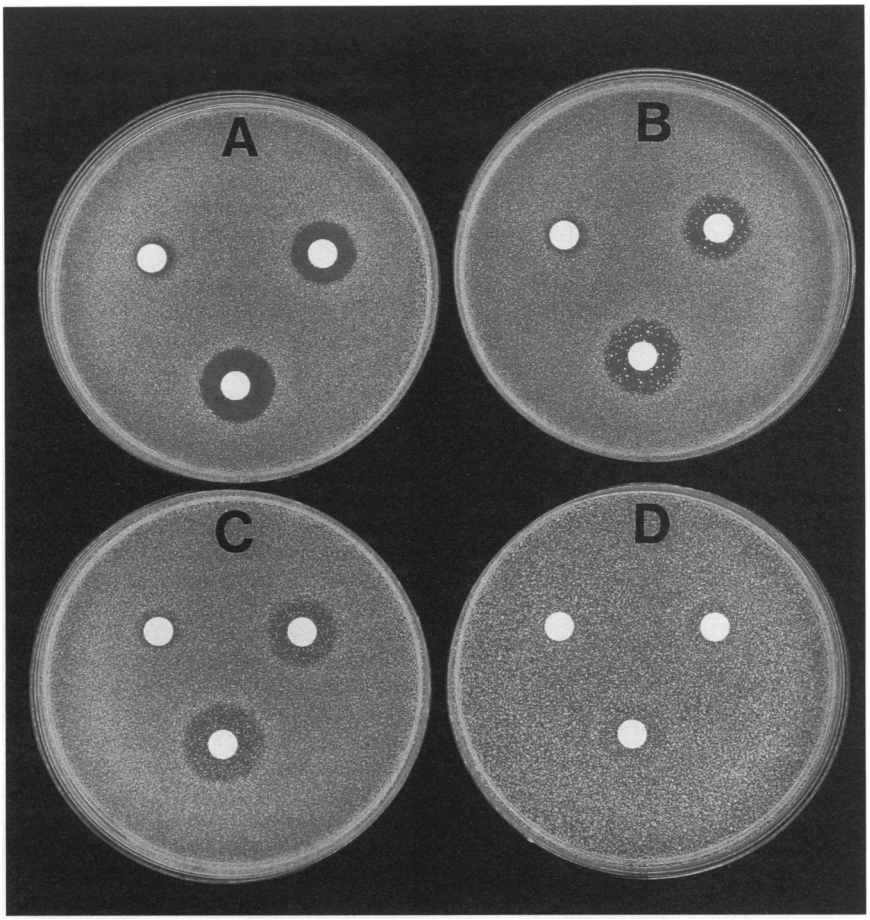


FIG. 7. Stabilization of Cln2 elevates resistance to and accelerates recovery from pheromone-induced cell cycle arrest. A yeast strain (YPH499) was transformed with a low-copy-number (*CEN*) vector, pRS314 (51) (A), or with the same vector expressing from the *CLN2* promoter either normal *CLN2* (pSS1) (B), *CLN2ΔPEST* (pSS37) (C), or *CLN2T* (pSS35) (D). Samples of each culture were plated in soft agar, overlaid with sterile disks containing 1 μg (upper left), 5 μg (upper right), or 10 μg (lower) synthetic α factor, and incubated at 30°C for 36 to 48 h.

that the steady-state level of Cln2 produced from that construct appeared to be lower in *MAT***a** cells exposed to the mating pheromone α factor than in control cells, suggesting that pheromone action might enhance the rate of Cln2 breakdown (58). To look more directly at the effect of pheromone treatment on the rate of Cln2 turnover, we performed pulse-chase experiments on *MAT***a** strains that were induced to express Cln2 from p*GAL1-CLN2* and then preincubated in the presence or absence of α factor. Regardless of whether cells were exposed to α factor for either 10 or 30 min before initiation of radiolabeling, there was no detectable change in the rate of Cln2 degradation during the subsequent chase period compared with that seen in the control cells (Fig. 8A). Essentially identical experiments were carried out to examine whether pheromone treatment affected the decay rate of hTKΔ40-Cln2; again, no increase or decrease was observed (data not shown). Thus, Cln2 appears to be a constitutively unstable protein, and treatment with α factor does not increase its rate of degradation.

It has also been reported that, when arrested in $G_1$ by shift of a strain carrying a temperature-sensitive *cdc28* mutation to the restrictive temperature, cells expressing Cln2 from the chromosomal *CLN2* locus accumulate this protein, as judged by immunoblotting (60). However, in our hands, pulse-chase analysis showed that the rate of degradation of hTKΔ40-Cln2 expressed from heterologous promoters was unaffected when cells carrying various $cdc28^{ts}$ alleles (including *cdc28-4* and *cdc28-9*) were shifted to the restrictive temperature (data not shown). We have also examined the rate of Cln2 and hTK-Cln2 degradation at other points in the cell cycle. When a $cdc21^{ts}$ (thymidylate synthase-deficient) mutant (2) was arrested during S phase by a shift to the nonpermissive temperature (37°C), the rate of Cln2 turnover was the same as that observed in the growing cells left at the permissive temperature (26°C) (data not shown), and this half-life was essentially identical to the half-life we observed for Cln2 in other asynchronous cultures. Similarly, when a $cdc15^{ts}$ (protein kinase-deficient) mutant (52a) was arrested during M phase by a shift to the nonpermissive temperature (37°C), the rate of hTK-Cln2 turnover was the same as that observed in the growing cells left at the permissive temperature (26°C) (data not shown), and this half-life was essentially identical to that we observed for hTK-Cln2 in other asynchronous cultures. These results provide further support for the conclusion that Cln2 destruction is a constitutive process.

**The *CDC34* gene product is not required for hTKΔ40-Cln2 or Cln2 breakdown in vivo.** Conjugation to ubiquitin is involved in the degradation of M phase cyclins and other proteins in animal cells (13); it has also been implicated in targeting various classes of proteins for destruction in *S.*

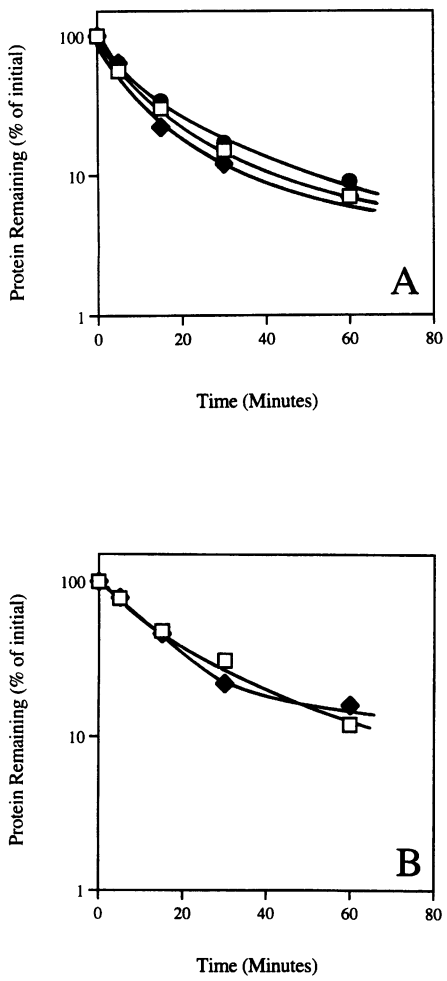


FIG. 8. Rate of Cln2 degradation under various conditions. (A) Effect of pheromone treatment. Strain DK499 (*MAT***a** *sst1*) carrying p*GAL1-CLN2* was induced to express Cln2 by incubation for 2 h in 2% galactose and then exposed to α factor for either 10 min (solid diamonds) or 30 min (solid circles) or left untreated (open squares) prior to initiation of the pulse-chase regimen, which was conducted as described in the legend to Fig. 5. (B) Effect of a *cdc34*$^{ts}$ mutation. A strain (YL10-1) carrying the *cdc34-2* mutation and harboring p*GAL1-CLN2* was induced to express Cln2 by incubation in 2% galactose and was shifted to the restrictive temperature (37°C) for 2 h (solid diamonds) or left at the permissive temperature (26°C) for 2 h (open squares) prior to initiation of the pulse-chase regimen, which was conducted as described in the legend to Fig. 5.

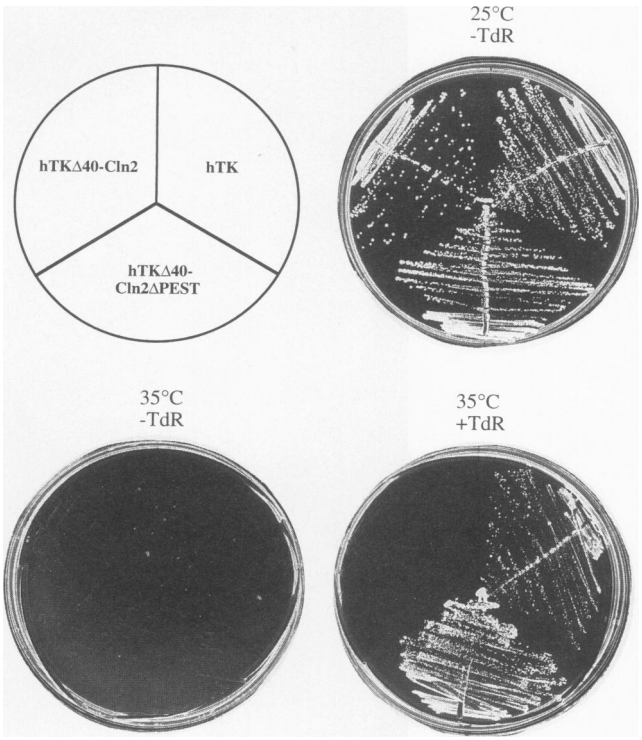


FIG. 9. Complementation of thymidylate deficiency in vivo by hTK and hTK derivatives. Individual colonies of a yeast strain (YSS21) carrying a temperature-sensitive mutation (*cdc21-1*) in the structural gene for thymidylate synthase and harboring a plasmid expressing either hTK (right), hTKΔ40-Cln2 (left), or hTKΔ40-Cln2ΔPEST (bottom), were streaked on SCGlc-Leu medium either lacking (-TdR) or containing (+TdR) 100 μg of thymidine per ml at either the permissive (25°C) or restrictive (35°C) temperature, as indicated. The particular colony of the hTK-containing cells that was streaked on the thymidine-containing plate at 35°C had apparently become petite; it is known that mitochondrial DNA replication is especially sensitive to dTMP deficiency (33).

*cerevisiae* (12). More than 10 different ubiquitin-conjugating enzymes (UBCs) have been identified in *S. cerevisiae* (23). The *CDC34* gene encodes UBC3, whose function is required for completion of the $G_1$-to-S transition (14, 37), the period just after the time when Cln2 is needed. Hence, one possible explanation for the blockade of cell cycle progression observed in *cdc34* mutants at the restrictive temperature might be an inability to remove Cln2 and/or other $G_1$ cyclins. Therefore, we examined the stability of Cln2 and hTKΔ40-Cln2 in strains carrying temperature-sensitive mutations in the *CDC34* gene by pulse-chase analysis. In strains carrying either the leaky *cdc34-1* allele (data not shown) or the tight *cdc34-2* allele (Fig. 8B), the rate of turnover of Cln2 was virtually the same at the restrictive temperature (37°C) as at the permissive temperature (26°C). Similarly, the turnover of hTKΔ40-Cln2 was unaffected in the *cdc34* mutants, regardless of the temperature (data not shown). Although these results do not rule out the possibility that Cln2 degradation proceeds via a ubiquitin-mediated pathway, our findings do suggest that the *CDC34* gene product (UBC3) is not necessary for degradation of this $G_1$ cyclin.

**A genetic method for examining the instability of PEST-containing proteins in vivo.** As an additional means to assess the stability in vivo of the various hTK constructs we generated, we examined their ability to support the growth of a thymidylate synthase-deficient yeast strain on thymidine-containing medium. For this purpose, we used a strain that carries a temperature-sensitive mutation (19) in the structural gene for thymidylate synthase (*CDC21/TMP1*) (2), which is unable to grow at the nonpermissive temperature (35°C) because no dTMP, an essential precursor for DNA synthesis, can be made (3). When the plasmid expressing full-length hTK was introduced into this strain, the cells were able to grow at 35°C, provided that thymidine was supplied to the growth medium (Fig. 9). In contrast, as expected from the low steady-state level (Fig. 4) and rapid turnover (Fig. 5) of the hTKΔ40-Cln2 chimera, the resulting low level of TK activity present in cells expressing hTKΔ40-Cln2 detected in vitro (Fig. 3) was not

sufficient to permit the growth of the mutant cells on thymidine-containing medium at 35°C (Fig. 9). However, in agreement with the greater stability of the hTKΔ40-Cln2ΔPEST chimera observed by the other methods we used (Fig. 3 to 5), cells expressing the hTKΔ40-Cln2ΔPEST protein were able to grow under these conditions (Fig. 9). The finding that hTKΔ40-Cln2 does not support the growth of a *cdc21* mutant whereas hTKΔ40-Cln2ΔPEST does provides a positive selection for identifying chromosomal mutations that are able to enhance the stability of the hTK-Cln2 chimera. As will be described in more detail elsewhere, cellular mutations isolated on this basis also affect the pattern of Cln2 breakdown in vivo (43c).

## DISCUSSION

Cln2 is an unstable protein of low abundance (56, 60). The finding that constitutive expression of Cln2 or its close homolog Cln1 has no dramatic effect on cell growth or division suggests that the protein can be rapidly degraded at any point in the cell cycle (28, 41, 58). As one approach to address the mechanism of $G_1$ cyclin degradation, we asked whether the sequences responsible for the instability of Cln2 could be localized within the polypeptide and whether such sequences would be capable of conferring an equal degree of instability upon an otherwise highly stable protein. Toward this end, we elected to use gene fusions to a reporter enzyme whose abundance could be readily monitored in vivo and in vitro and whose variation in level might have sufficient physiological consequences to provide the basis for a genetic selection. For this purpose, we chose the monomeric enzyme hTK. We found, first, that hTK is functional in *S. cerevisiae* and is a very stable protein. Furthermore, in contrast to what is observed in animal cells, both the full-length protein and a small truncation, hTKΔ40, were equally stable. We found, further, that fusion of only the 178 C-terminal amino acids of the 545-residue Cln2 protein onto the C terminus of hTKΔ40 was sufficient to convert the otherwise stable hTKΔ40 enzyme into a highly unstable molecule. Moreover, the half-life and other features of the degradation of the hTKΔ40-Cln2 chimera resembled in every respect tested the behavior of authentic Cln2. These findings indicate that major determinants of the instability of this $G_1$ cyclin are, in fact, found in 178 (or fewer) amino acids of its C-terminal domain. Our results are consistent with previous genetic findings (17), in which a mutation (*CLN2-1*) that substituted the C-terminal 170 residues of Cln2 with a heterologous sequence acted like a dominant hyperactive allele (17). Our observations suggest that the most likely explanation for the dominant hyperactive effect of the *CLN2-1* allele is that the altered protein cannot be efficiently degraded. In direct confirmation of this conclusion, we found by two independent criteria that the product of an allele containing a precise truncation of the same 175-residue segment (*CLN2T*) was, in fact, a more stable protein than full-length Cln2. Likewise, mutations in *CLN3* that truncate the C terminus of the protein also create dominant hyperactive alleles (*CLN3-1* and *CLN3-2*) (8, 31), and the truncated proteins appear to be more stable than normal Cln3 (57).

The short half-life of the hTKΔ40-Cln2 chimera appears to be due exclusively to some signal(s) for rapid degradation within the appended Cln2 sequence and not to an indirect effect of that sequence (for example, causing misfolding of the whole molecule and subsequent proteolysis), for several reasons. First, by every criterion that we tested, both the hTKΔ40 truncated protein and the hTK-LacZ60 chimera (24) were just as stable and just as active as enzymes as hTK itself, demonstrating that neither the folding nor the catalytic activity of hTK is intrinsically sensitive to perturbations at its carboxyl-terminal end. Second, strains expressing hTKΔ40-Cln2 had low but readily detectable TK activity that paralleled the level of the hTKΔ40-Cln2 polypeptide, indicating that the hybrid protein was able to fold properly. Third, removal of a small segment (37 amino acids) of the 178-residue Cln2 portion of the hTKΔ40-Cln2 chimera significantly stabilized the molecule.

The turnover rate of hTKΔ40-Cln2 ($t_{1/2} \approx 12$ min) was markedly higher than that of hTK ($t_{1/2} \gg 2$ h) and quite similar to, but somewhat lower than, that of authentic Cln2 ($t_{1/2} \approx 8$ min). Likewise, Hochstrasser and Varshavsky (20) found that fusion of otherwise stable β-galactosidase to the very unstable MATα2 repressor created a chimeric protein that was very unstable but that this MATα2-LacZ hybrid nevertheless had a half-life three times longer than that of MATα2 itself.

Because our results showed that the carboxyl-terminal region of Cln2 harbors the main *cis*-acting signals that determine its rate of degradation, we attempted to further delineate the limits and nature of those signals. In particular, we wanted to address the importance of the PEST sequences as determinants of protein instability. PEST motifs have been identified in many unstable proteins (42), but evidence that these elements directly target proteins for destruction has been lacking. Within the C-terminal region of Cln2 that was attached to hTKΔ40 and that greatly destabilized this protein, residues 375 to 408 form the most strikingly PEST-like sequence. Indeed, when this segment was deleted from either hTKΔ40-Cln2 or Cln2 itself, the half-life of the resulting proteins was significantly extended. Thus, at least one of the PEST motifs within the Cln2 tail clearly contributes in a substantial way to the overall ability of the C-terminal domain to act as an instability determinant. However, removal of this major PEST element did not convert hTKΔ40-Cln2 or Cln2 to dramatically more stable proteins. Because other PEST-containing stretches remain in the Cln2 portion of hTKΔ40-Cln2ΔPEST and, likewise, other PEST-like stretches exist both upstream and downstream of the deletion in Cln2ΔPEST, it seems likely that all of these elements may influence the stability of the Cln2 molecule. If the contributions of these sequences are redundant and additive, removal of any single PEST motif would not be expected to provide a pronounced enhancement of stability, as was observed. This notion is also consistent with our finding that the Cln2T protein, which lacks the entire C terminus (175 residues), was somewhat more stable than Cln2ΔPEST. Correspondingly, removal of the major PEST segment from hTKΔ40-Cln2 led to a somewhat greater increase in half-life than did the same deletion from Cln2. Also consistent with the view that PEST elements may be additive in their effects on protein stability was our finding that the major, 37-residue PEST segment from Cln2 was unable, by itself, to confer a dramatic destabilization on hTKΔ40. Thus, that particular PEST motif can be, at best, only part of the signal necessary for demarcating instability.

Nonetheless, our results establish unequivocally that the carboxyl-terminal region of Cln2 harbors the main *cis*-acting signals that determine its instability. We also wanted to address, with both hTKΔ40-Cln and Cln2 as probes, whether Cln2 breakdown is a regulated or a constitutive process. The yeast mating pheromone α factor causes *MAT***a** cells to arrest in the $G_1$ phase of the cell cycle and also causes a dramatic drop in *CLN1* and *CLN2* transcript levels and in Cln2 protein levels (Cln1 was not examined) (60). This regulation is thought to be mediated by the *FAR1* gene product, a negative regulator of Cln2 (6). Far1 is a substrate for one of the protein kinases,

Fus3, activated by the mating-pheromone signaling pathway (11). In its phosphorylated state, Far1 binds to and inhibits the catalytic activity of $p34^{CDC28}$-Cln2 complexes (35, 55). In all likelihood, this inhibition prevents the autocatalytic stimulation of *CLN2* transcription (32), because it would presumably block phosphorylation (and activation) of the Swi4/Swi6 transcription factor by the $p34^{CDC28}$/Cln2 complex. Because Cln2 is a highly unstable protein, as we have shown here, in the absence of continuous *CLN2* mRNA synthesis the level of Cln2 should fall precipitously in response to pheromone, as has been observed. On the other hand, the recent finding that expression of Cln2 from an unregulated promoter does not cause resistance to pheromone (58) was taken as suggestive evidence that Far1 might also act posttranscriptionally, perhaps by increasing the rate of Cln2 turnover; in support of this idea, immunoblot analysis showed that the steady-state level of constitutively expressed Cln2 stayed high in a *far1* mutant treated with pheromone (58). However, we addressed this issue directly by examining the decay rate of Cln2 (and hTKΔ40-Cln2) by pulse-chase analysis and could find no evidence whatsoever to indicate that the turnover of Cln2 (or hTKΔ40-Cln2) is enhanced following exposure of *MAT***a** cells to α factor.

The system we have developed also has allowed us to begin to explore the effect of mutations in known genes that are likely to have a role in $G_1$ cyclin degradation. One of the best candidates for such a function was the product of the *CDC34* gene, which is UBC3, an enzyme that is known to be involved in intracellular protein degradation and whose activity is required late in $G_1$. However, our data indicate that Cdc34 is not required for Cln2 degradation. The stability of another $G_1$ cyclin, Cln3, also appears to be unaffected by *cdc34* mutations (57). Since yeast cells contain multiple UBCs (23) and since the degradation of an individual protein can involve more than one UBC (7), our results do not rule out the possibility that the $G_1$ cyclins are degraded by a ubiquitin-dependent mechanism. Indeed, in our immunoblot and pulse-chase analyses, multiple higher-molecular-weight forms of both hTKΔ40-Cln2 and Cln2 were frequently observed, consistent with polyubiquitination. However, attempts to determine if these species can cross-react with anti-ubiquitin antibodies have been unsuccessful, at least with commerically available antisera (Sigma) and other antisera we obtained as gifts from various sources (Arthur Haas, Department of Biochemistry, Medical College of Wisconsin, Milwaukee; Victor Fried, Department of Cell Biology and Anatomy, New York Medical College, Valhalla). Furthermore, for all of the derivatives of hTKΔ40 that contain Cln2 sequences (hTKΔ40-Cln2, hTKΔ40-Cln2ΔPEST, and hTKΔ40-ClnPEST), a doublet band was always observed. The higher-molecular-weight species of the pair is a phosphoprotein, as judged by the fact that it becomes radioactive when cells are metabolically labeled with $^{32}PO_4^{3-}$ (43a). It is not clear, however, whether this posttranslational modification is obligatory for the subsequent destruction of the protein. Since the rate of hTKΔ40-Cln2 degradation was unaffected when various $cdc28^{ts}$ mutants were shifted to the nonpermissive temperature and since the doublet bands still persisted under these conditions, it seems unlikely that $p34^{CDC28}$ is the protein kinase responsible for this modification.

Although the difference in half-life between hTKΔ40-Cln2 and hTKΔ40Cln2ΔPEST was only modest, this threefold difference in stability had dramatic consequences in vivo—the hTKΔ40-Cln2 chimera could not support the growth of thymidylate synthase-deficient cells on thymidine medium, whereas the hTKΔ40-Cln2ΔPEST chimera could. This phenotype confirmed the conclusions derived from the enzymological, immunological, and biochemical assays performed on the same molecules. Thus, the use of hTK as a reporter enzyme provided a very sensitive assay for protein levels in vivo. This phenotypic difference could be exploited further, because it also provides a basis for a genetic selection for chromosomal mutations that enhance the stability of hTKΔ40-Cln2 and, presumably, the endogenous $G_1$ cyclins. Mutants totally defective in their ability to degrade $G_1$ cyclins may be very sick or inviable, particularly if all $G_1$ cyclins are degraded by a common mechanism or if the machinery used for $G_1$ cyclin degradation is also required for the degradation of other proteins that may be toxic to cells if accumulated at too high a level. However, since only a threefold increase in hTKΔ40-Cln2 levels is required for survival under the selection conditions we have devised, it should be possible to identify mutants that are only partially defective in their ability to degrade $G_1$ cyclins. Indeed, using this approach, we have obtained several mutants which permit the growth of a $cdc21^{ts}$ strain at the restrictive temperature in a thymidine-dependent manner when hTKΔ40-Cln2 is the sole source of TK activity in the cell (43c). In several of these mutants, overexpression of *CLN2* is toxic even at intermediate temperatures, suggesting that turnover of authentic Cln2 is also affected. Immunoblot analysis confirms that in several of these mutants the pattern of Cln2 breakdown is markedly altered. Further characterization of such mutations may provide insight into the mechanism by which PEST sequences target proteins for destruction and the machinery that is responsible for $G_1$ cyclin degradation.

## ACKNOWLEDGMENTS

We thank Tom Kelly and Mike Kauffman for providing hTK constructs and anti-hTK antibodies; Bret Benton for providing YEp352G; Curt Wittenberg for providing various *cdc28* strains; Mark Goebl for providing the *cdc34-2* strain; Doug Koshland for providing the *cdc15-1* strain; David Kaim for constructing DK499; Bill Courchesne and Dan Mytelka for initially isolating *CLN2* clones and Karl Kuchler for preparing anti-Cln2 antiserum; Akio Toh-e for providing the *pho80*::*HIS3* construction; Sylvia Sanders, Dori Hosobuchi, Nina Salama, and Dave Feldheim for giving advice on cell labeling and lysis; Randy Schekman for permitting us to use his PhosphorImager; Mallory Haggart, Mike Moore, and Jim Onuffer for synthesizing oligonucleotides; and Owen Fields, Henrik Dohlman, Karl Kuchler, and other members of the Thorner laboratory for providing additional materials and advice.

This work was supported by a predoctoral fellowship from the Howard Hughes Medical Institute (to S.R.S.), by predoctoral traineeship GM07232 from the National Institutes of Health (to K.B.H.), by NIH research grant GM21841 (to J.T.), and by facilities provided by the Cancer Research Laboratory of the University of California, Berkeley.

## REFERENCES

1. **Benton, B. M., W.-K. Eng, J. J. Dunn, F. W. Studier, R. Sternglanz, and P. A. Fisher.** 1990. Signal-mediated import of bacteriophage T7 RNA polymerase into the *Saccharomyces cerevisiae* nucleus and specific transcription of target genes. Mol. Cell. Biol. **10**:353–360.
2. **Bisson, L., and J. Thorner.** 1977. Thymidine 5′-monophosphate-requiring mutants of *Saccharomyces cerevisiae* are deficient in thymidylate synthetase. J. Bacteriol. **132**:44–50.
3. **Bisson, L. F.** 1980. Studies on thymidylate metabolism in *Saccharomyces cerevisiae*. Ph.D. thesis. University of California, Berkeley.
4. **Bisson, L. F., and J. Thorner.** 1982. Mutations in the *PHO80* gene confer permeability to 5′-mononucleotides in *Saccharomyces cerevisiae*. Genetics **102**:341–359.
5. **Boeke, J. D., J. Trueheart, G. Natsoulis, and G. R. Fink.** 1987. 5′-Fluoroorotic acid as a selective agent in yeast molecular genetics. Methods Enzymol. **154**:164–175.
6. **Chang, F., and I. Herkowitz.** 1990. Identification of a gene

necessary for cell cycle arrest by a negative growth factor of yeast: *FAR1* is an inhibitor of a G1 cyclin, *CLN2*. Cell **63**:999–1011.
7. **Chen, P., P. Johnson, T. Sommer, S. Jentsch, and M. Hochstrasser.** 1993. Multiple ubiquitin-conjugating enzymes participate in the *in vivo* degradation of the yeast MATα2 repressor. Cell **74**:357–369.
8. **Cross, F. R.** 1988. *Daf1*, a mutant gene affecting size control, pheromone arrest, and cell cycle kinetics of *Saccharomyces cerevisiae*. Mol. Cell. Biol. **8**:4675–4684.
9. **Cross, F. R.** 1990. Cell cycle arrest caused by *CLN* gene deficiency in *Saccharomyces cerevisiae* resembles START-I arrest and is independent of the mating pheromone signaling pathway. Mol. Cell. Biol. **10**:6482–6490.
10. **Dreyfuss, G., S. A. Adam, and D. Y. Choi.** 1984. Physical change in cytoplasmic messenger ribonucleoproteins in cells treated with inhibitors of mRNA transcription. Mol. Cell. Biol. **4**:415–423.
11. **Elion, E. A., B. Satterberg, and J. E. Kranz.** 1993. FUS3 phosphorylates multiple components of the mating signal transduction cascade: evidence for STE12 and FAR1. Mol. Biol. Cell **4**:495–510.
12. **Finley, D.** 1992. The yeast ubiquitin system, p. 539–581. *In* E. W. Jones, J. R. Pringle, and J. R. Broach (ed.), The molecular and cellular biology of the yeast *Saccharomyces*: gene expression. Cold Spring Harbor Laboratory Press, Cold Spring Harbor, N.Y.
13. **Glotzer, M., A. W. Murray, and M. W. Kirschner.** 1991. Cyclin is degraded by the ubiquitin pathway. Nature (London) **349**:132–138.
14. **Goebl, M. G., J. Yochem, S. Jentsch, J. P. McGrath, A. Varshavsky, and B. Byers.** 1988. The yeast cell cycle gene *CDC34* encodes a ubiquitin-conjugating enzyme. Science **241**:1331–1335.
15. **Grivell, A. R., and J. F. Jackson.** 1968. Thymidine kinase: evidence for its absence from *Neurospora crassa* and some other microorganisms and the relevance of this to the specific labelling of deoxyribonucleic acid. J. Gen. Microbiol. **54**:307–317.
16. **Hadwiger, J. A., and S. I. Reed.** 1990. Nucleotide sequence of the *Saccharomyces cerevisiae CLN1* and *CLN2* genes. Nucleic Acids Res. **18**:4025.
17. **Hadwiger, J. A., C. Wittenberg, H. E. Richardson, M. De Barros Lopes, and S. I. Reed.** 1989. A family of cyclin homologs that control the $G_1$ phase in yeast. Proc. Natl. Acad. Sci. USA **86**: 6255–6259.
18. **Harlow, E., and D. Lane.** 1988. Antibodies: a laboratory manual. Cold Spring Harbor Laboratory, Cold Spring Harbor, N.Y.
19. **Hartwell, L. H.** 1973. Three additional genes required for deoxyribonucleic acid synthesis in *Saccharomyces cerevisiae*. J. Bacteriol. **115**:966–974.
20. **Hochstrasser, M., and A. Varshavsky.** 1990. In vivo degradation of a transcriptional regulator: the yeast α2 repressor. Cell **61**:697–708.
21. **Hosobuchi, M., T. Kreis, and R. Schekman.** 1992. *SEC21*, a gene required for ER to Golgi protein transport, encodes a subunit of a yeast cotamer. Nature (London) **360**:603–605.
22. **Ito, H., Y. Fukuda, K. Murata, and A. Kimura.** 1983. Transformation of intact yeast cells treated with alkali cations. J. Bacteriol. **153**:163–168.
23. **Jentsch, S.** 1992. The ubiquitin-conjugation system. Annu. Rev. Genet. **26**:179–207.
23a. **Kaim, D., and J. Thorner.** Unpublished results.
24. **Kauffman, M. G., and T. J. Kelly.** 1991. Cell cycle regulation of thymidine kinase: residues near the carboxyl terminus are essential for the specific degradation of the enzyme at mitosis. Mol. Cell. Biol. **11**:2538–2546.
25. **Koerner, T. J., J. E. Hill, A. M. Myers, and A. Tzagaloff.** 1991. High-expression vectors with multiple cloning sites for construction of *trpE* fusion genes: pATH vectors. Methods Enzymol. **194**: 477–490.
26. **Kuchler, K., H. G. Dohlman, and J. Thorner.** 1993. The a-factor transporter (*STE6* gene product) and cell polarity in the yeast *Saccharomyces cerevisiae*. J. Cell Biol. **120**:1203–1215.
27. **Lee, L.-S., and Y.-C. Cheng.** 1976. Human deoxythymidine kinase. I. Purification and general properties of the cytoplasmic and mitochondrial isozymes derived from blast cells of acute myelocytic leukemia. J. Biol. Chem. **251**:2600–2604.
28. **Lew, D. J., V. Dulic, and S. I. Reed.** 1991. Isolation of three novel human cyclins by rescue of G1 cyclin (Cln) function in yeast. Cell **66**:1197–1206.
29. **Martin, G. A., D. Viskochil, G. Bollag, P. C. McCabe, W. J. Crosier, H. Haubruck, L. Conroy, R. Clark, P. O'Connell, R. M. Cawthon, M. A. Innis, and F. McCormick.** 1990. The GAP-related domain of the neurofibromatosis type 1 gene product interacts with *ras* p21. Cell **63**:843–849.
30. **Mendenhall, M. D., C. A. Jones, and S. I. Reed.** 1987. Dual regulation of the yeast CDC28-p40 protein kinase complex: cell cycle, pheromone, and nutrient limitation effects. Cell **50**:927–935.
31. **Nash, R., G. Tokiwa, S. Anand, K. Erickson, and A. B. Futcher.** 1988. The *WHI1*$^+$ gene of *Saccharomyces cerevisiae* tethers cell division to cell size and is a cyclin homolog. EMBO J. **7**:4335–4346.
32. **Nasmyth, K.** 1993. Control of the yeast cell cycle by the Cdc28 protein kinase. Curr. Opin. Cell Biol. **5**:166–179.
33. **Newlon, C. S., and W. L. Fangman.** 1975. Mitochondrial DNA synthesis in cell cycle mutants of *Saccharomyces cerevisiae*. Cell **5**:423–428.
34. **Nurse, P.** 1990. Universal control mechanism regulating onset of M-phase. Nature (London) **344**:503–506.
35. **Peter, M., A. Gartner, J. Horecka, G. Ammerer, and I. Herskowitz.** 1993. FAR1 links the signal transduction pathway to the cell cycle machinery in yeast. Cell **73**:747–760.
36. **Pines, J.** 1993. Cyclins and cyclin-dependent kinases: take your partners. Trends Biochem. Sci. **18**:195–197.
37. **Pringle, J. R., and L. H. Hartwell.** 1981. The *Saccharomyces cerevisiae* cell cycle, p. 97–142. *In* J. N. Strathern, E. W. Jones, and J. R. Broach (ed.), The molecular biology of the yeast *Saccharomyces*: life cycle and inheritance. Cold Spring Harbor Laboratory, Cold Spring Harbor, N.Y.
38. **Reed, S. I.** 1980. The selection of *S. cerevisiae* mutants defective in the start event of cell division. Genetics **95**:561–577.
39. **Reed, S. I.** 1991. G1-specific cyclins: in search of an S-phase-promoting factor. Trends Genet. **7**:95–99.
40. **Reneke, J. E., K. J. Blumer, W. E. Courchesne, and J. W. Thorner.** 1988. The carboxy-terminal segment of the yeast α-factor receptor is a regulatory domain. Cell **55**:221–234.
41. **Richardson, H. E., C. Wittenberg, F. Cross, and S. I. Reed.** 1989. An essential G1 function for cyclin-like proteins. Cell **59**:1127–1133.
42. **Rogers, S., R. Wells, and M. Rechsteiner.** 1986. Amino acid sequences common to rapidly degraded proteins: the PEST hypothesis. Science **234**:364–368.
43. **Rose, M. D., F. Winston, and P. Hieter.** 1990. Methods in yeast genetics. A laboratory course manual. Cold Spring Harbor Laboratory Press, Cold Spring Harbor, N.Y.
43a. **Salama, S.** Unpublished results.
43b. **Salama, S., K. Kuchler, and J. Thorner.** Unpublished results.
43c. **Salama, S., and J. Thorner.** Unpublished results.
44. **Sambrook, J., E. F. Fritsch, and T. Maniatis.** 1989. Molecular cloning: a laboratory manual. Cold Spring Harbor Laboratory Press, Cold Spring Harbor, N.Y.
45. **Sanger, G. S., S. Nicklen, and A. R. Coulson.** 1977. DNA sequencing with chain-terminating inhibitors. Proc. Natl. Acad. Sci. USA **74**:5463–5467.
46. **Sclafani, R. A., and W. L. Fangman.** 1984. Yeast gene *CDC8* encodes thymidylate kinase and is complemented by herpes virus thymidine kinase gene, *TK*. Proc. Natl. Acad. Sci. USA **81**:5821–5825.
47. **Sclafani, R. A., and W. L. Fangman.** 1986. Thymidine utilization by TUT mutants and facile cloning of mutant alleles by plasmid conversion in *S. cerevisiae*. Genetics **114**:753–767.
48. **Sherley, J. L., and T. J. Kelly.** 1988. Human cytosolic thymidine kinase. Purification and physical characterization of the enzyme from HeLa cells. J. Biol. Chem. **263**:375–382.
49. **Sherley, J. L., and T. J. Kelly.** 1988. Regulation of human thymidine kinase during the cell cycle. J. Biol. Chem. **263**:8350–8358.
50. **Sherman, F.** 1991. Getting started with yeast. Methods Enzymol. **194**:3–21.
51. **Sikorski, R. S., and P. Hieter.** 1989. A system of shuttle vectors and yeast host strains designed for efficient manipulation of DNA in

*Saccharomyces cerevisiae*. Genetics **122:**19–27.

52. **Solomon, M. J.** 1993. Activation of the various cyclin/cdc2 protein kinases. Curr. Opin. Cell Biol. **5:**180–186.

52a. **Schweitzer, B., and P. Philippsen.** 1991. *CDC15*, an essential cell cycle gene in *Saccharomyces cerevisiae*, encodes a protein kinase domain. Yeast **7:**265–273.

53. **Toh-e, A., and T. Shimauchi.** 1986. Cloning and sequencing of the *PHO80* gene and *CEN15* of *Saccharomyces cerevisiae*. Yeast **2:** 129–139.

54. **Towbin, H., T. Staehelin, and J. Gordon.** 1979. Electrophoretic transfer of proteins from polyacrylamide gels to nitrocellulose sheets: procedure and some applications. Proc. Natl. Acad. Sci. USA **76:**4350–4354.

55. **Tyers, M., and B. Futcher.** 1993. Far1 and Fus3 link the mating pheromone signal transduction pathway to three $G_1$-phase Cdc28 kinase complexes. Mol. Cell. Biol. **13:**5659–5669.

56. **Tyers, M., G. Tokiwa, and B. Futcher.** 1993. Comparison of the *Saccharomyces cerevisiae* $G_1$ cyclins. EMBO J. **12:**1955–1968.

57. **Tyers, M., G. Tokiwa, R. Nash, and B. Futcher.** 1992. The Cln3-Cdc28 kinase complex of *S. cerevisiae* is regulated by proteolysis and phosphorylation. EMBO J. **11:**1773–1784.

58. **Valdivieso, M. H., K. Sugimoto, K.-Y. Jahng, P. M. B. Fernandes, and C. Wittenberg.** 1993. *FAR1* is required for posttranscriptional regulation of *CLN2* gene expression in response to mating pheromone. Mol. Cell. Biol. **13:**1013–1022.

58a. **Wittenberg, C.** Personal communication.

59. **Wittenberg, C., and S. I. Reed.** 1988. Control of the yeast cell cycle is associated with assembly/disassembly of the cdc28 protein kinase complex. Cell **54:**1061–1072.

60. **Wittenberg, C., K. Sugimoto, and S. I. Reed.** 1990. G1-specific cyclins of S. cerevisiae: cell cycle periodicity, regulation by mating pheromone and association with the p34 CDC28 protein kinase. Cell **62:**225–237.

61. **Yon, J., and M. Fried.** 1989. Precise gene fusion by PCR. Nucleic Acids Res. **17:**4895.